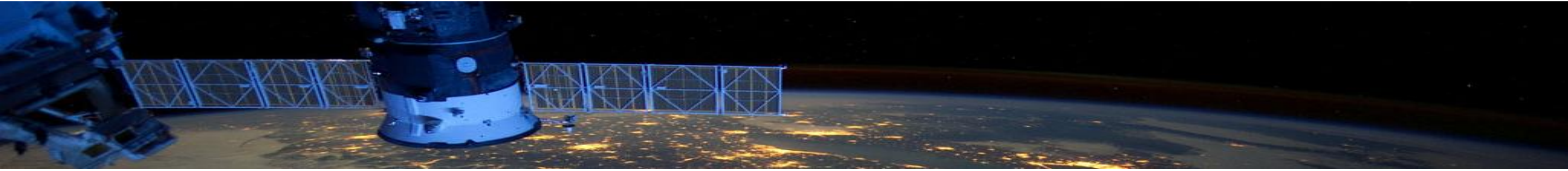

Towards a Global Climatological Spread F Model

Krishnendu Sekhar Paul[1], Haris Haralambous[1,2]

[1]Frederick Research Center (FRC), Nicosia, Cyprus

[2]Frederick University, Nicosia, Cyprus

The International Reference Ionosphere and NeQuick – Improving the Representation of the Real-Time Ionosphere, ICTP, Trieste, Italy, 28 September–10 October 2025.

INTRODUCTION

- Midlatitude nighttime ionograms frequently exhibit diffuse F-region traces, commonly referred to as midlatitude **Spread F (SF),** which can persist from minutes to several hours (Bowman 1996).

- *A primary driver of SF in the midlatitude F-region is spatial perturbations in electron density, often triggered by gravity waves (GW).*

- Bowman (1996) reported that *SF occurrence rates are inversely correlated with solar flux, potentially due to variations in Upper Atmosphere Neutral Particle Density (UA-NPD) affecting the amplitude of Traveling Ionospheric Disturbances (TIDs).*

- *TIDs result from GW coupling between the neutral atmosphere and the ionosphere (Bowman 1996), causing ionospheric tilts that can lead to SF when their amplitudes are sufficiently large. Therefore* the link between SF occurrence and UA-NPD can be explained by the influence of neutral density on TID amplitudes.

INTRODUCTION

SF can be broadly **categorized into two types** based on the manifestation of diffused ionogram traces.

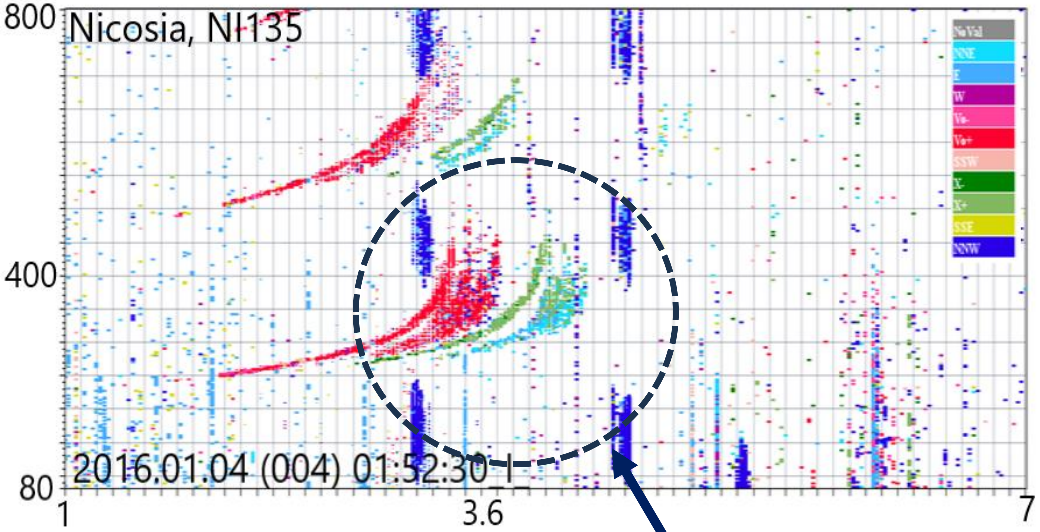

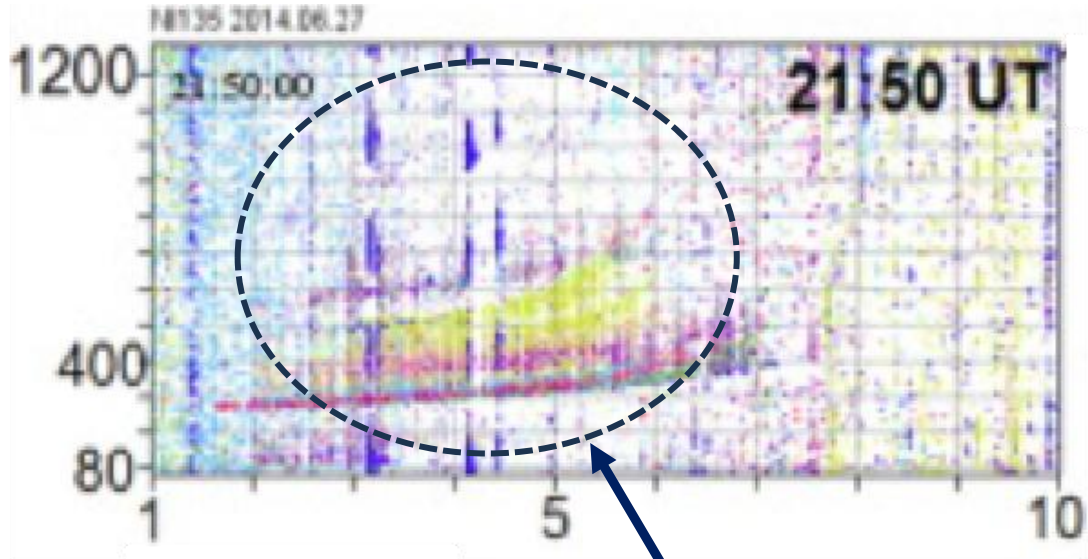

Frequency Spread F (FSF) when minimal spreading occurs at low frequencies, but diffused echoes are concentrated near the critical frequency of the F-region trace, indicating substantial trace spread in frequency (Hajkowicz 2007).

Range Spread F (RSF) characterized by diffused echoes appearing in the low-frequency segments (<2–2.5 MHz) of the F-region traces. These echoes extend approximately 10 km or more beyond the true range of the main echo, indicating substantial trace spread in range (Hajkowicz 2007).

INTRODUCTION

Observation of the Spread F occurrence over Nicosia, Athens and Pruhonice during 2009, 2015 and 2016 (Paul et al. 2018)

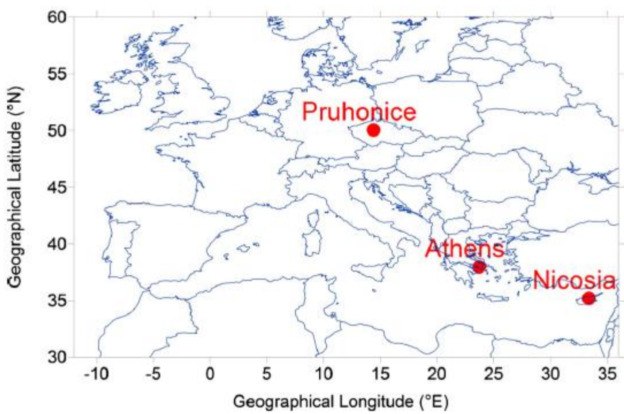

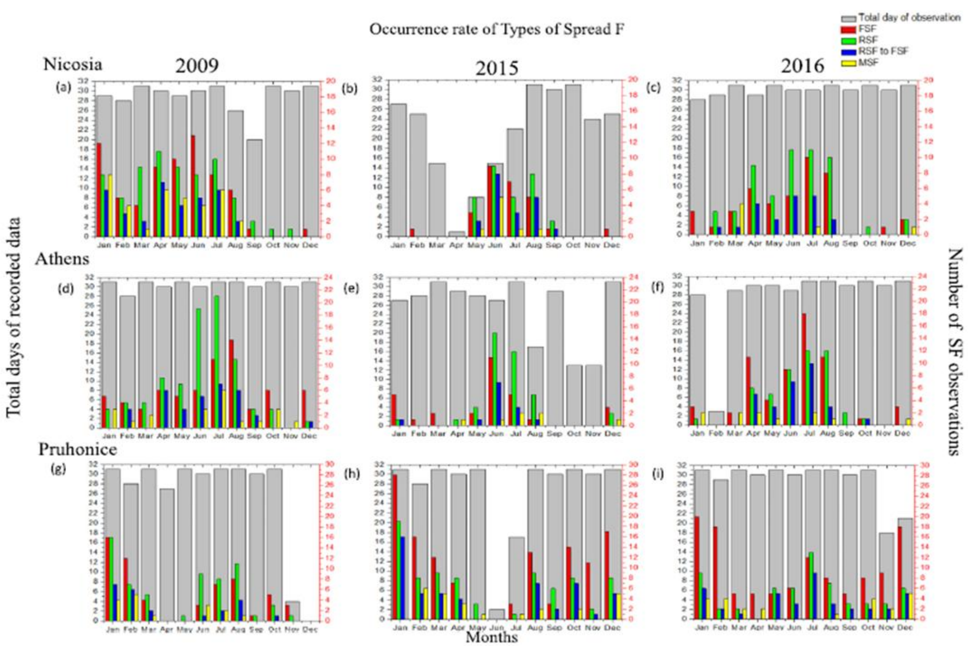

Monthly variation of different spread F types observed (a) from Nicosia on 2009 (b) from Nicosia on 2015 (c) from Nicosia on 2016 (d) from Athens on 2009 (e) from Athens on 2015 (f) from Athens on 2016 (g) from Pruhonice on 2009 (h) from Pruhonice on 2015 (i) from Pruhonice on 2016.

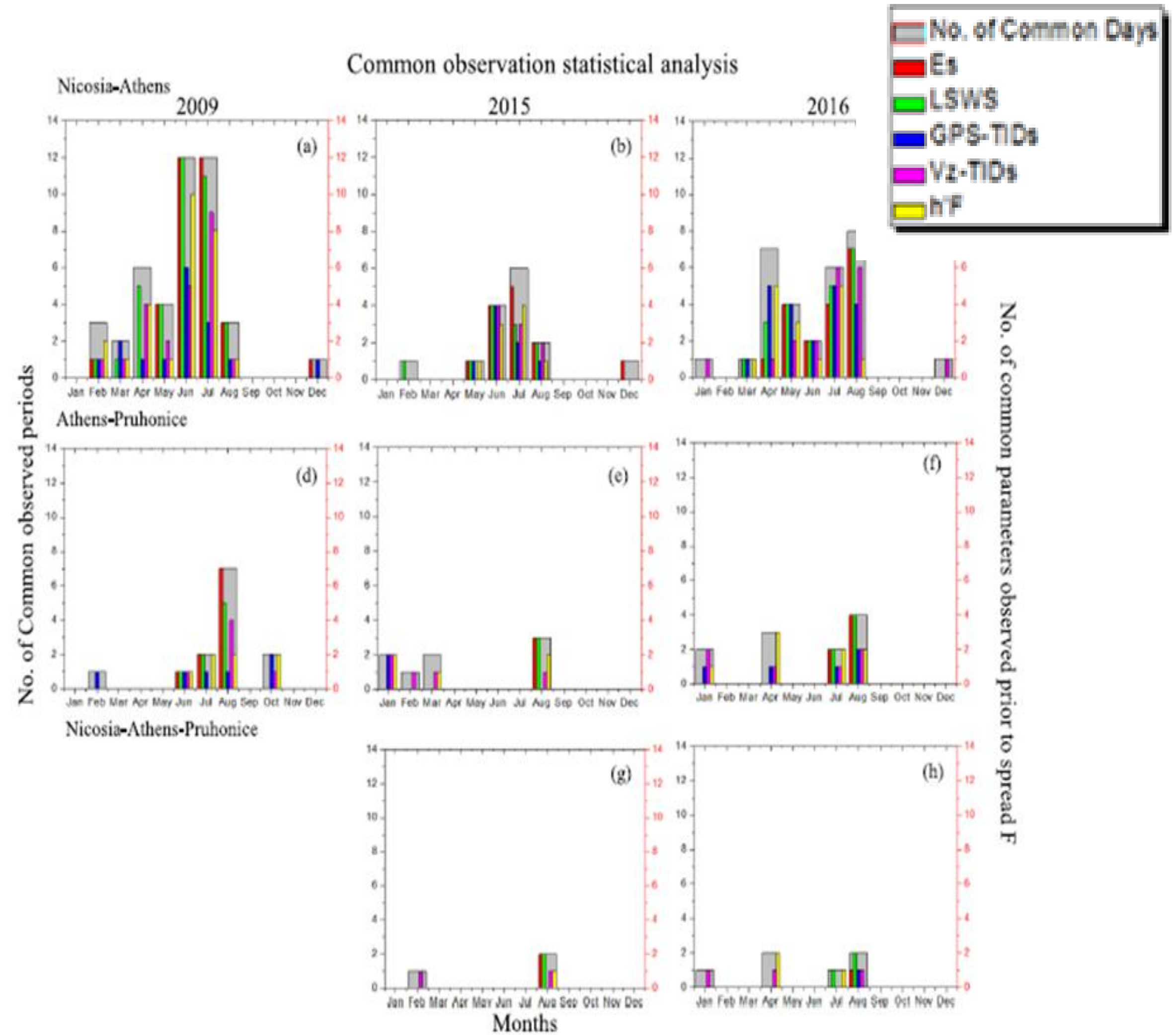

Statistical analysis for different parameters and precursors observed prior to the common spread F observation from (a) Nicosia and Athens on 2009 (b) Nicosia and Athens on 2015 (c) Nicosia and Athens on 2016 (d) Athens and Pruhonice on 2009 (e) Athens and Pruhonice on 2015 (f) Athens and Pruhonice on 2016 (g) Nicosia, Athens and Pruhonice on 2015 (h) Nicosia, Athens and Pruhonice on 2016.

INTRODUCTION

Spread F occurrence Moscow-Nicosia 20

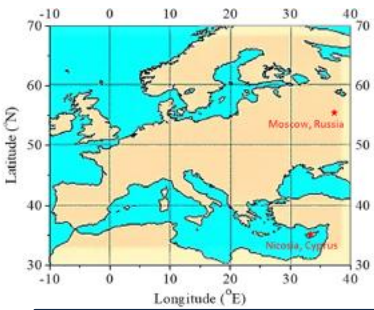

Number of spread F cases observed over Moscow during 2009 to 2020 and number of spread F cases for which hmF2 > 300 km.

Year of observations	Number of spread F events observed per year	Spread F events for which hmF2 > 300 km
2009	222	222
2010	209	171
2011	207	207
2012	286	272
2013	283	276
2014	302	302
2015	299	298
2016	256	256
2017	296	255
2018	258	203
2019	223	156
2020	120	112

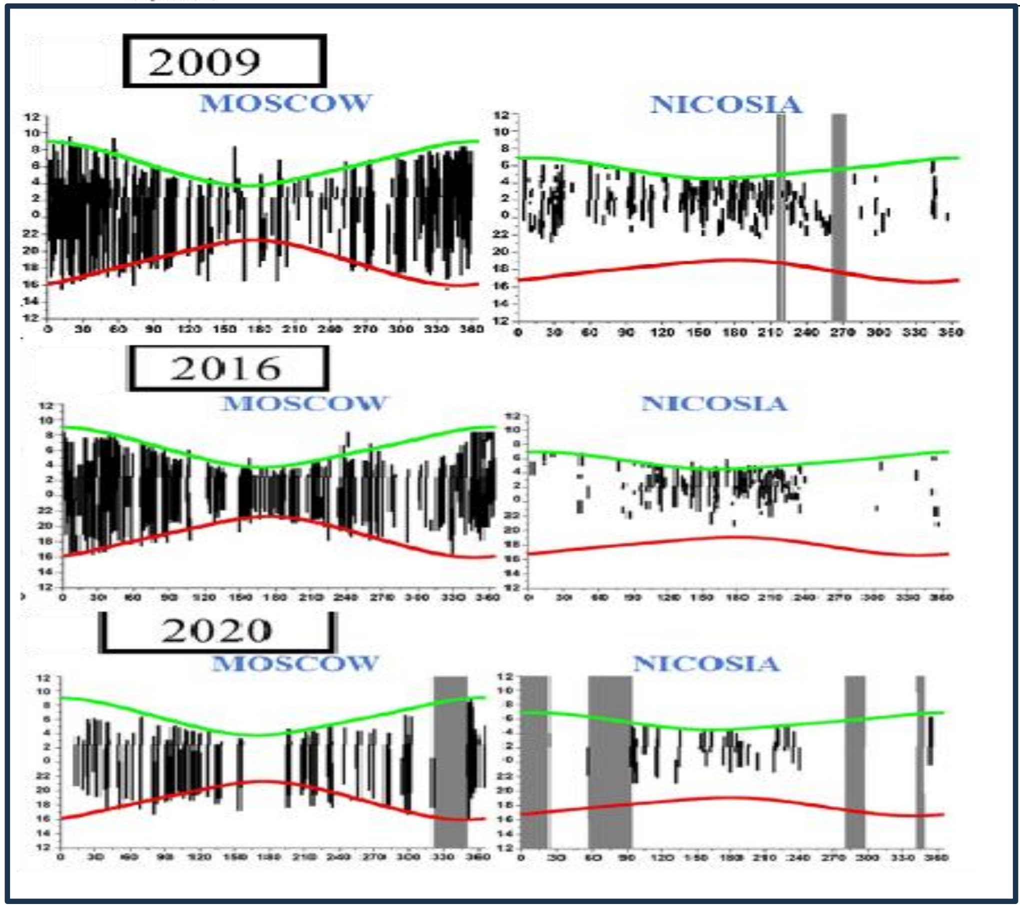

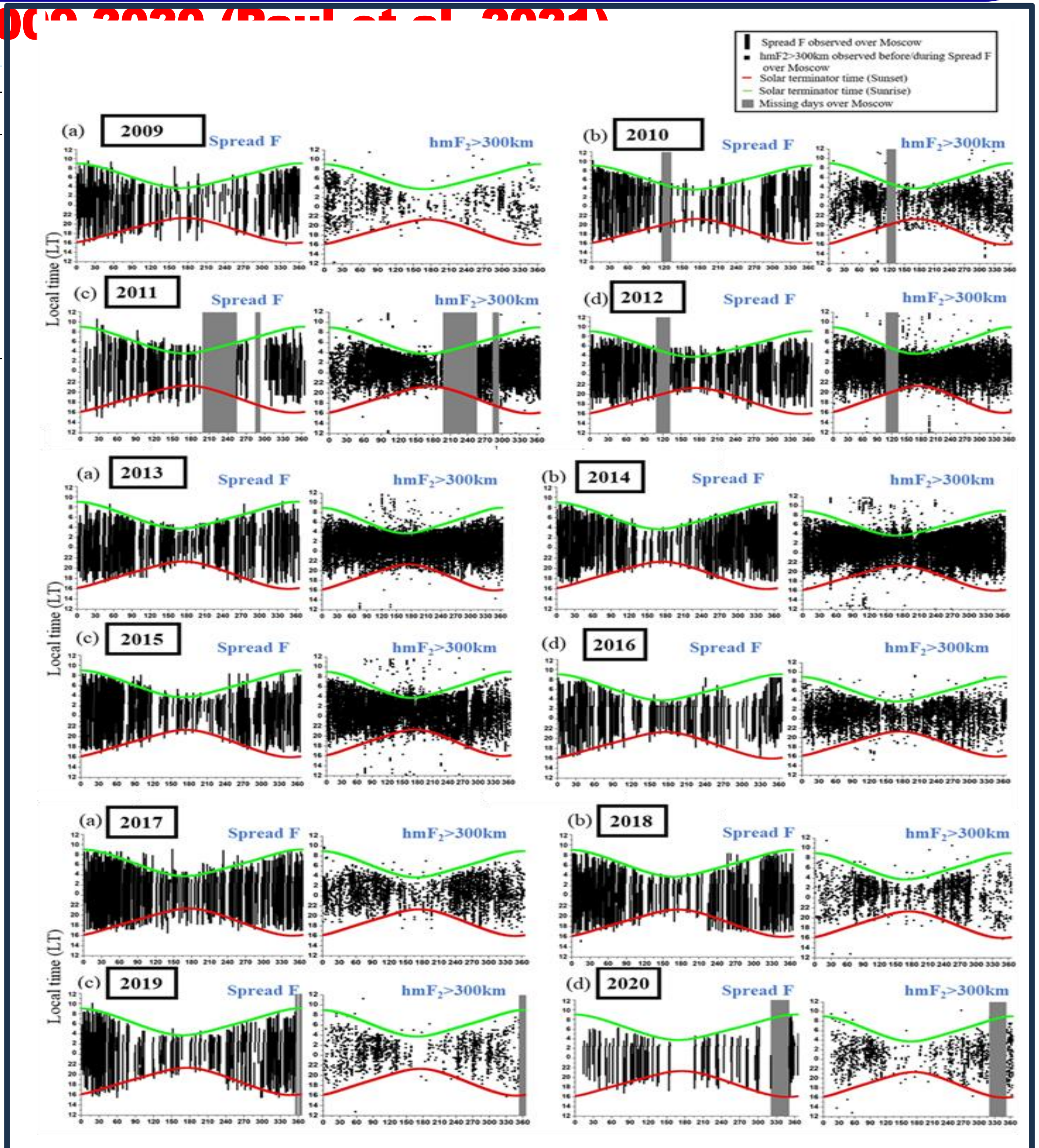

INTRODUCTION

***From the Auto-scaled datasets, we concentrated on two key characteristics*: QF and FF.**

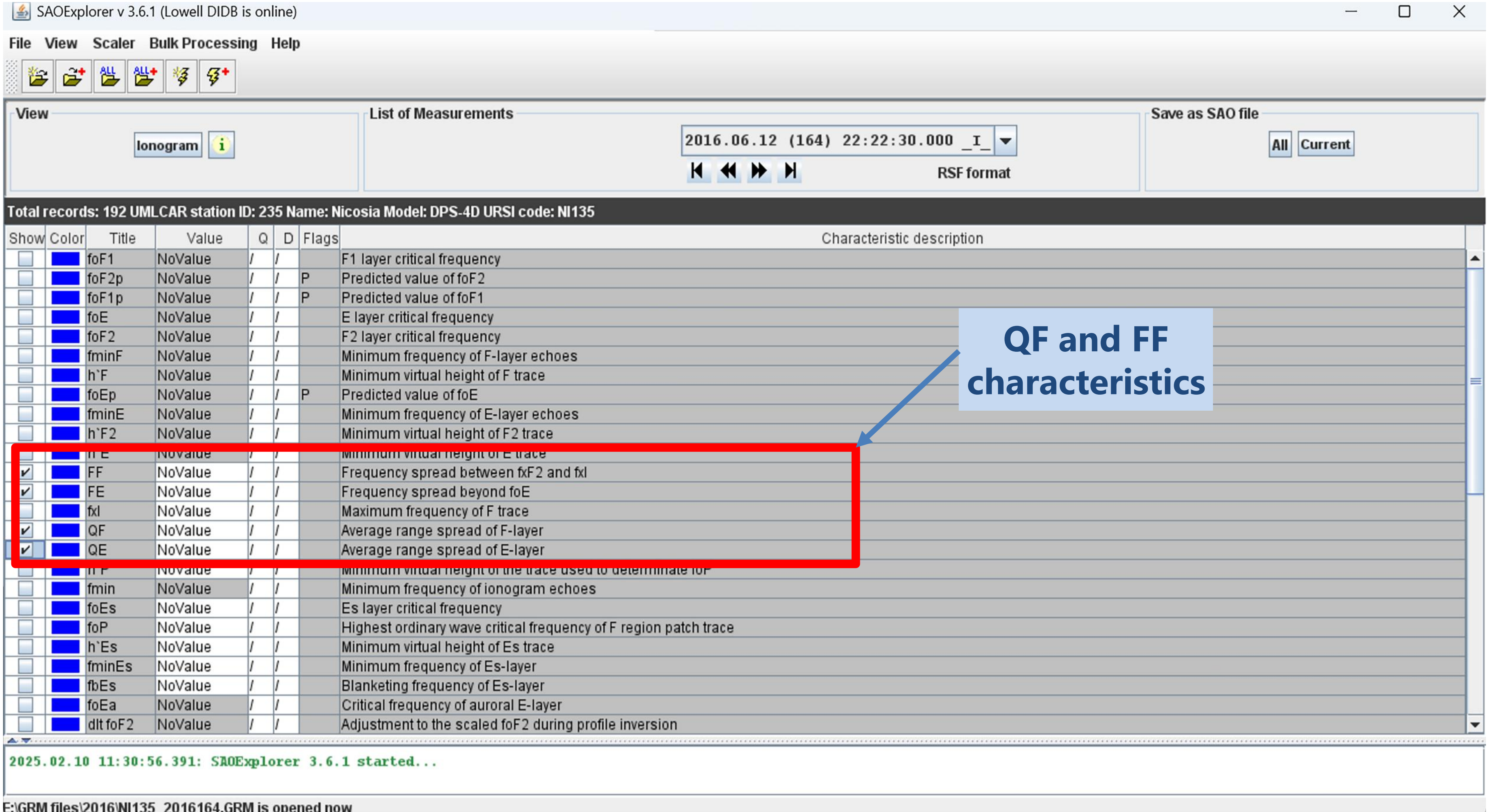

INTRODUCTION

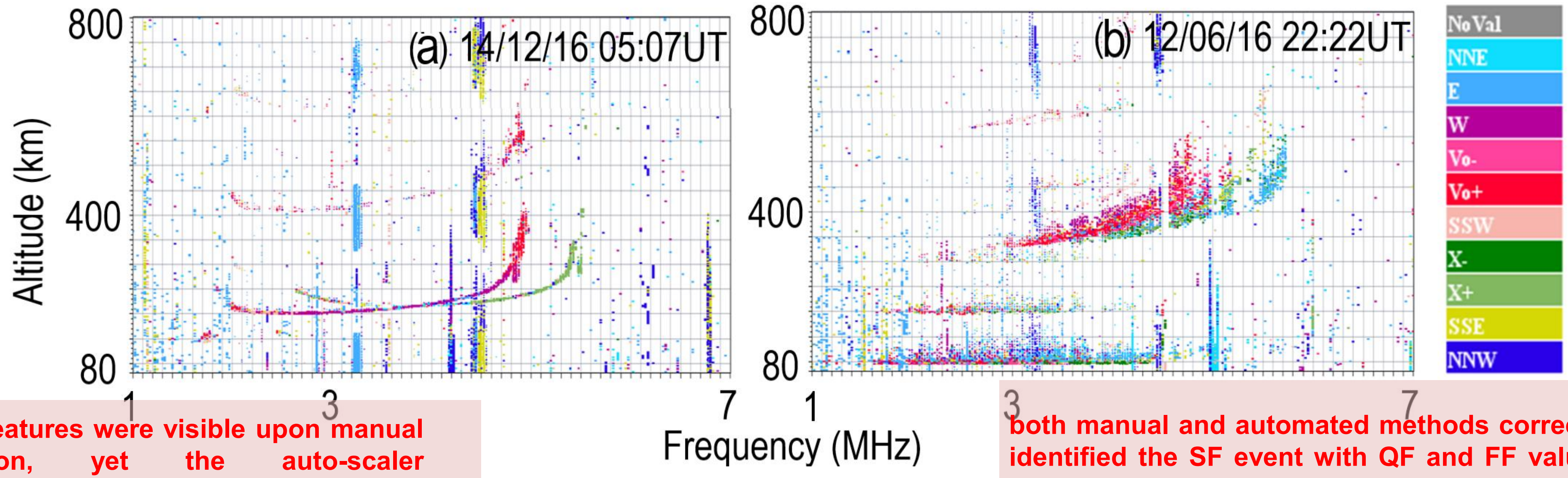

no SF features were visible upon manual evaluation, yet the auto-scaler inaccurately recorded a QF value of ~10km

both manual and automated methods correctly identified the SF event with QF and FF values (>10 km and >0.2 MHz, respectively

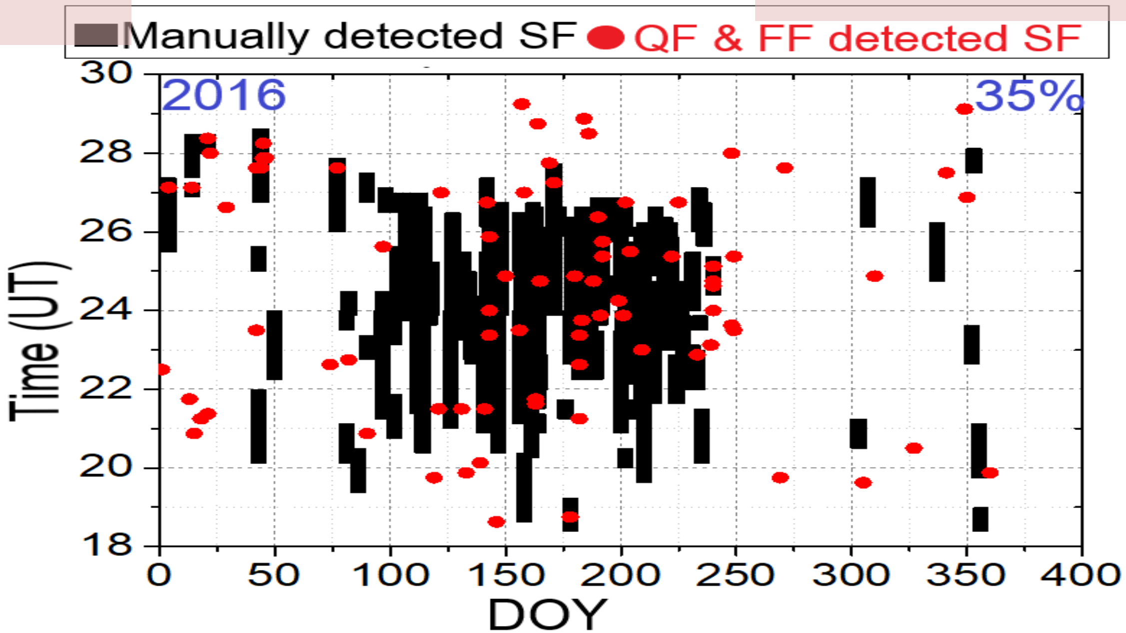

INTRODUCTION (Focus of the present study)

- To enhance detection reliability, *we developed a technique that combines ARTIST-derived SF indicators with ionospheric parameters known to act as indicators or drivers of SF*.

- This study evaluates the accuracy and consistency of our SF detection technique by comparing its outputs against manually identified SF occurrences at nine midlatitude ionospheric stations across Europe.

- The analysis utilizes a comprehensive dataset spanning from 2009 to 2021 and incorporates two key ionospheric parameters that act as key SF drivers —
  - **hmF2 uplifts in conjunction with the FF parameter to identify FSF events**,
  - **h′F fluctuations combined with the QF parameter to detect RSF events**.

- By contrasting the present detection with manually verified events, the study aims to determine the effectiveness of these parameters in reliably identifying SF phenomena.

Latitude Range	Stations	Latitude (°N)	Longitude (°E)	Manual SF detected years
35°–40°	Nicosia	35.03	33.16	2009–2010, 2013–2016, 2020–2021
	Athens	38	23.5	2009, 2015–2016
40°–45°	Rome	41.8	12.5	2017, 2020–2021
	Roquetes	40.8	0.5	2012–2021
50°–55°	Pruhonice	50	14.6	2009, 2015–2017, 2020–2021
	Dourbes	50.1	4.6	2017, 2020–2021
	Chilton	51.5	–0.6	2017, 2020–2021
55°–60°	Juliusruh	54.6	13.4	2017, 2020–2021
	Moscow	55.47	37.3	2009–2021

- To evaluate the SF detection method, we employed auto–scaled ionogram data obtained from the FastChar database hosted on the DIDBase platform (https://giro.uml.edu/didbase/scaled.php).

- These auto–scaled datasets were acquired for the same nine stations and over the same time interval as in the manual analysis.

- **From the auto–scaled ionograms, we considered four key parameters associated with SF detection: QF, FF, hmF2, and hF (h'F).**

- Notable data deficiencies were observed for the following stations and years: Chilton (2020), Pruhonice (2009 and 2020), Rome (2017), Athens (2009), and Nicosia (2020 and 2021).

- The SSN data were obtained from the **Solar Influences Data Analysis Center (SIDC)**, accessible at https://www.sidc.be/SILSO/datafiles

Analysis *(Automated SF detection)*

- To ensure data integrity in our analysis, we discarded:
  - **Excessive h'F fluctuations (Δh'F >400 km)**
  - **FF values exceeding 1 MHz**,
- To identify potential drivers for RSF events, we calculated h'F fluctuations (Δh'F) using the second–difference method.

For the present SF detection technique, we established the following criteria:

I. **QF > 0**: QF is considered latitude–independent and serves as a basic indicator of RSF activity.

II. ***a*** **< Δh′F < 400 km**: Δh′F exceeding a threshold value '*a*' strongly suggests the likelihood of RSF. The value of '*a*' (in km) is latitude–dependent, as SF occurrence depends on latitude.

III. **hmF2 >** ***b*** **for FF < 1 MHz**: We define '*b*'(in km) as a latitude–dependent threshold, beyond which the probability of FSF increases under the condition that FF remains within realistic limits (FF < 1 MHz).

IV. **FF >** ***c*** **and FF < 1 MHz, with hmF2 >** ***b***: we calculated a threshold '*c*' (in MHz), above which FF values pointed to confirmed FSF occurrence, particularly when accompanied by higher hmF2 values (hmF2 > *b*).

Analysis

Latitude zone	Stations Included	Threshold candidate	SF detection time
35°–40°N	Athens and Nicosia	Nicosia	18:00–06:00 UT
40°–45°N	Roquetes and Rome	Roquetes	16:00–07:00 UT
50°–55°N	Pruhonice, Dourbes and Chilton	Pruhonice	16:00–07:00 UT
55°–60°N	Moscow and Juliusruh	Moscow	14:00–08:00 UT

Analysis (Threshold Value estimation)

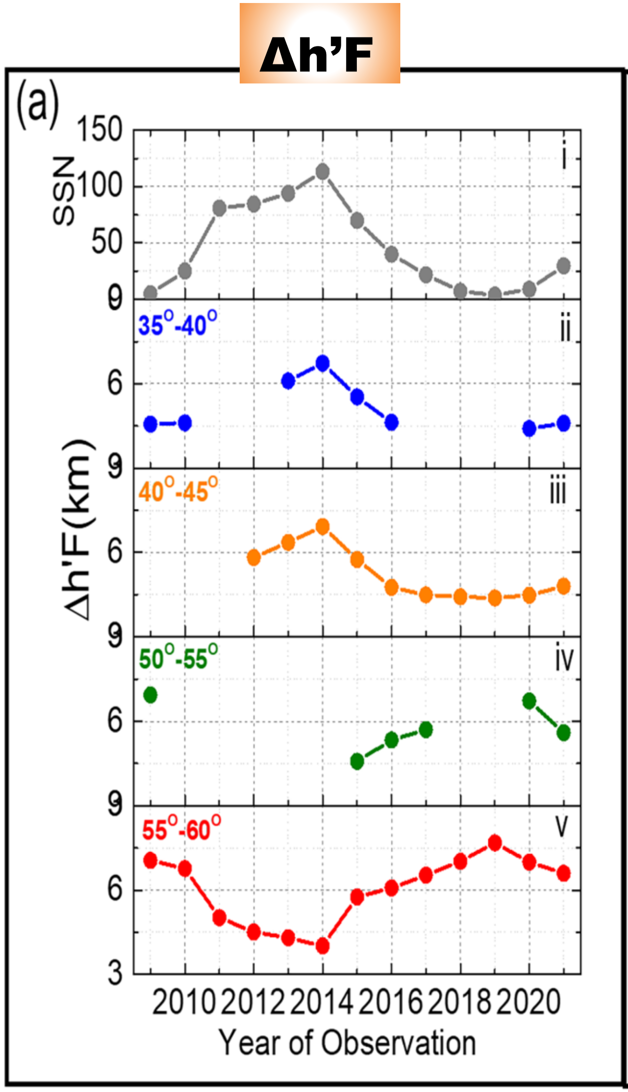

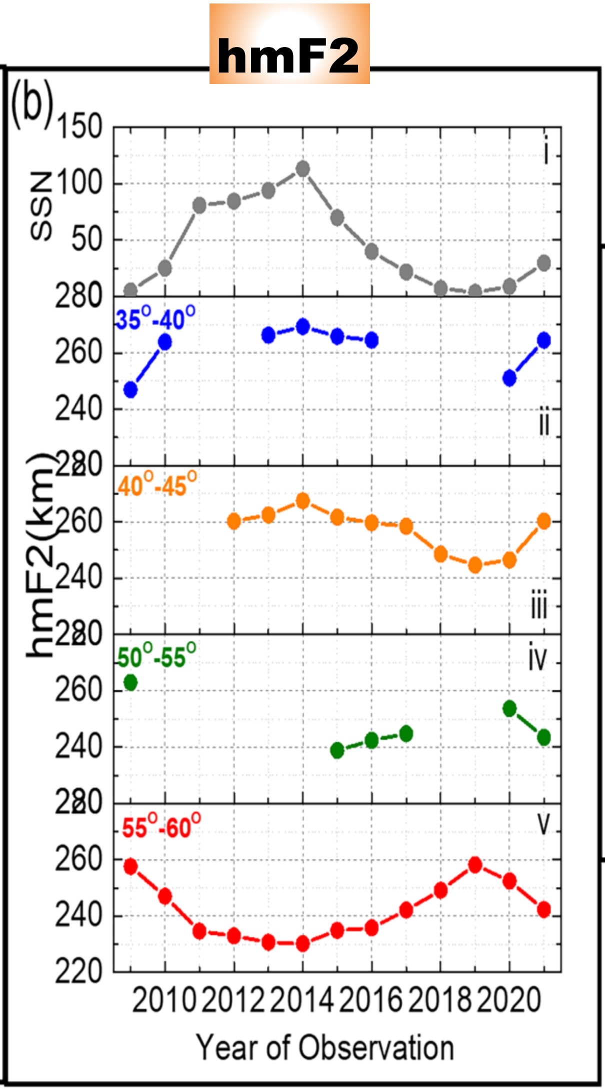

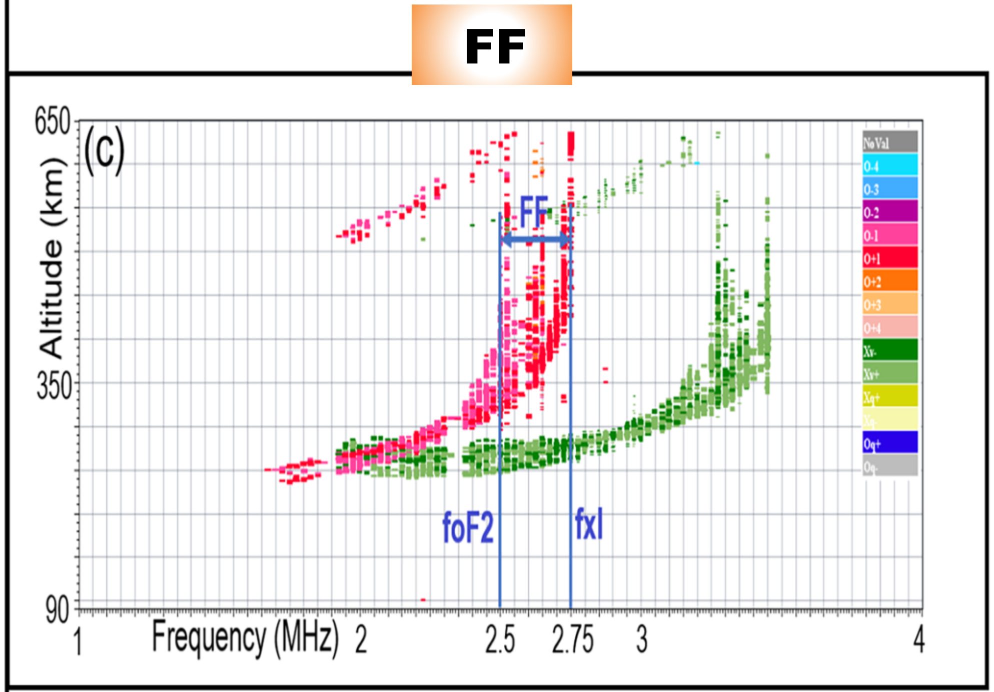

Paul et al (2025), Atmosphere

Analysis *(Manual SF detection)*

- For RSF detection (Hajkowicz, 2007), we identified distinct latitudinal variations in RSF occurrence.
- We adopted a criterion based on the vertical spread along the altitude axis. If the F-region trace exhibited a spreading range between 10 km and 50 km, we classified it as RSF.
- FSF events were identified based on horizontal spreading along the frequency axis. Specifically, ionograms exhibiting frequency spread in the range of 0.2 to 1 MHz were classified as FSF events.
- To ensure reliability in event classification, we imposed a temporal consistency condition: only those SF events that persisted across three or more consecutive ionograms—each separated by 5-minute intervals, corresponding to a minimum duration of 15 minutes (Paul et al. 2018, 2019, 2021, 2023, 2025)— were considered in this study.
- Any ionograms in which the spread Es layer blanketed or obscured the F-region trace were excluded from the analysis to avoid misclassification.
- To assess the performance of the detection algorithm, **we compared SF_P with SF_M. The accuracy of the prediction was quantified using**

$$CommonObs(\%) = \frac{SF_M \cap SF_P}{SF_P} \times 100$$

RESULTS *(55°–60°N latitude)*

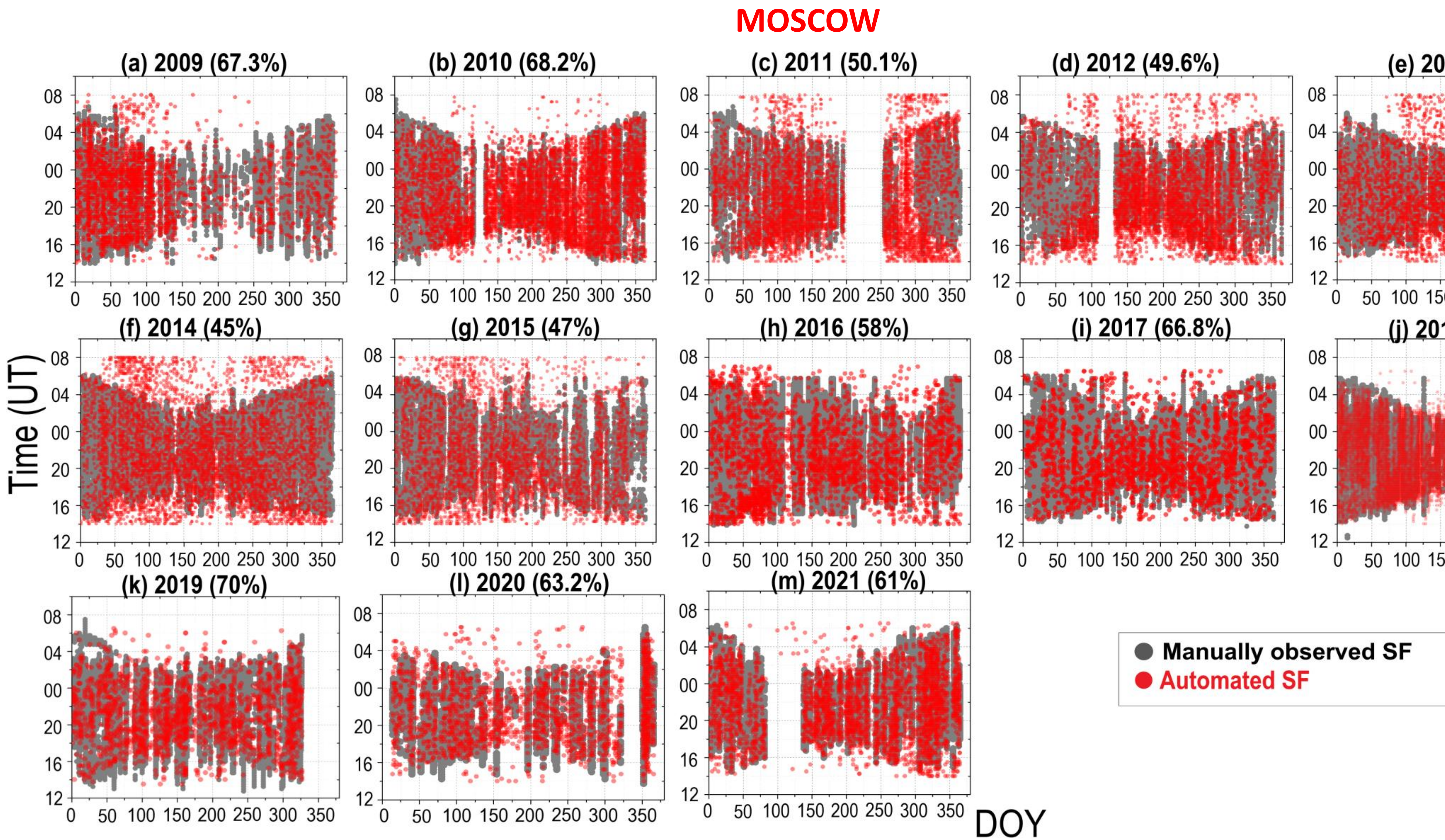

Paul et al (2025), Atmosphere

RESULTS *(55°–60°N latitude)*

JULIUSRUH

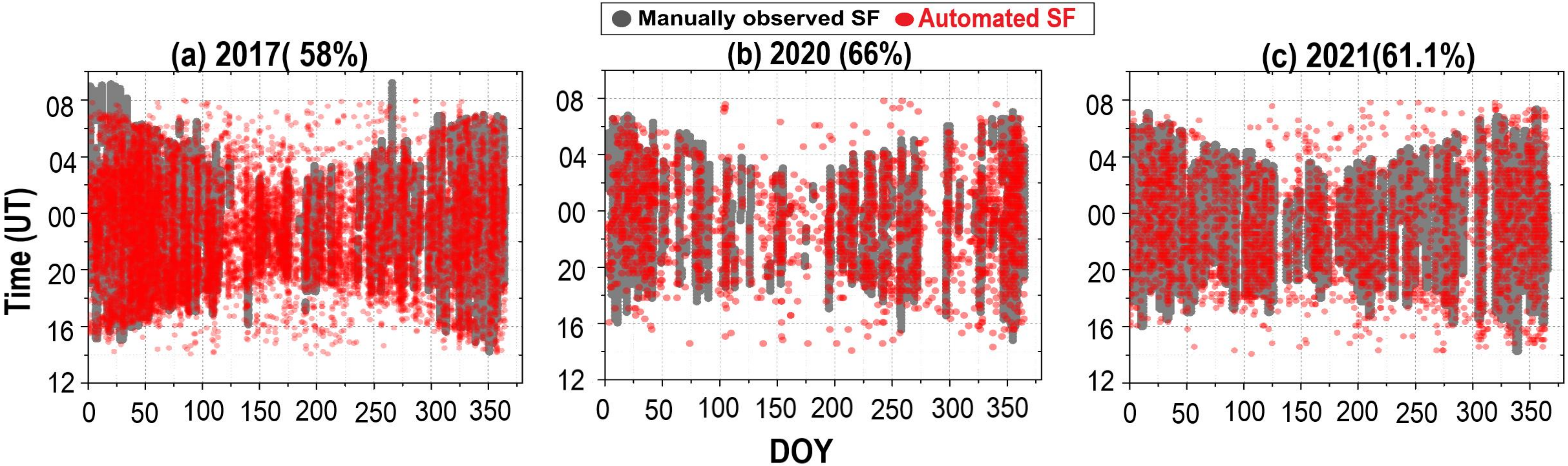

Paul et al (2025), Atmosphere

RESULTS *(50°–55°N latitude)*

CHILTON

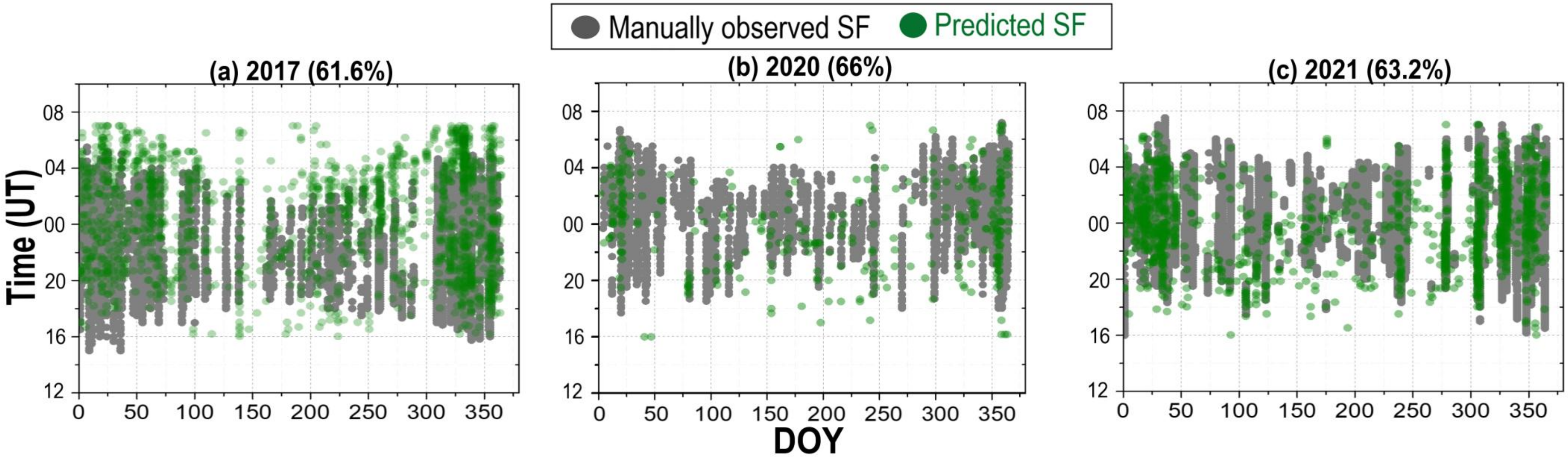

DOURBES

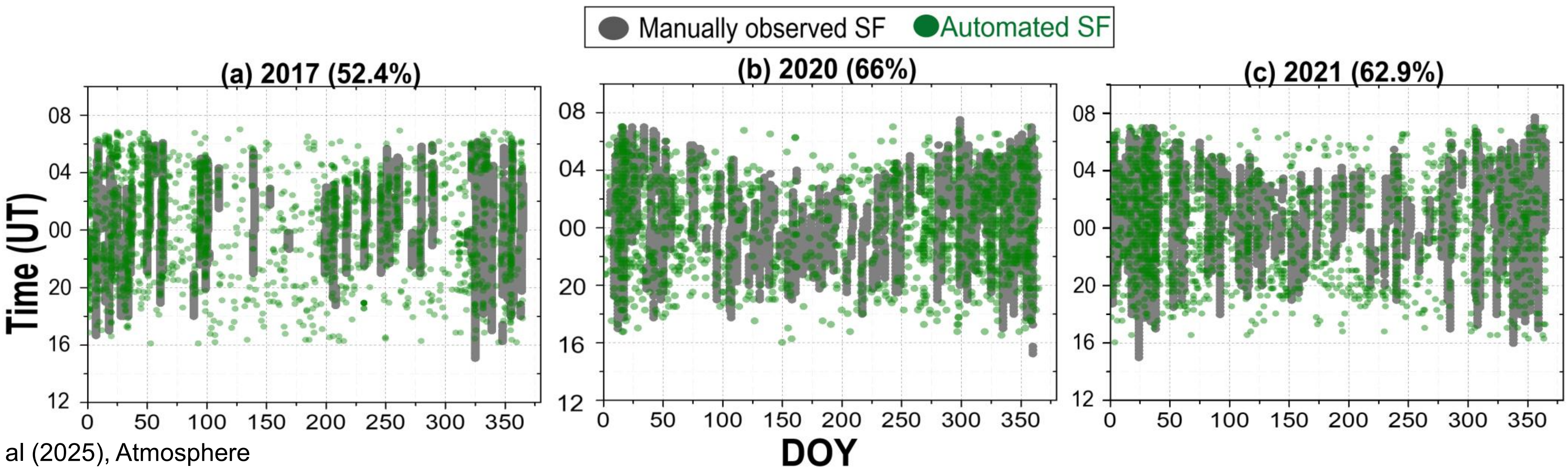

Paul et al (2025), Atmosphere

RESULTS *(50°–55°N latitude)*

PRUHONICE

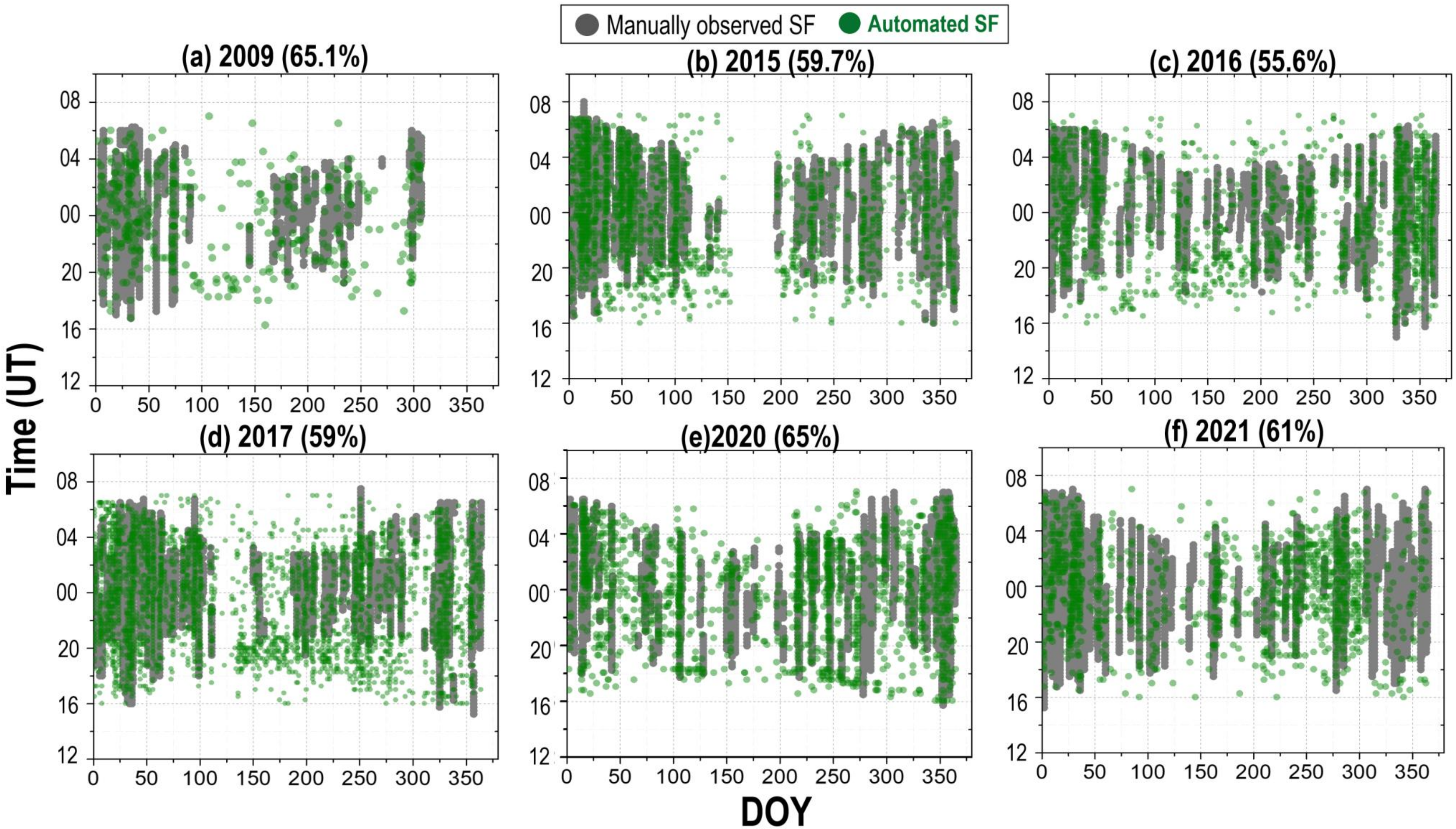

Paul et al (2025), Atmosphere

RESULTS *(40°–45°N latitude)*

ROQUETES

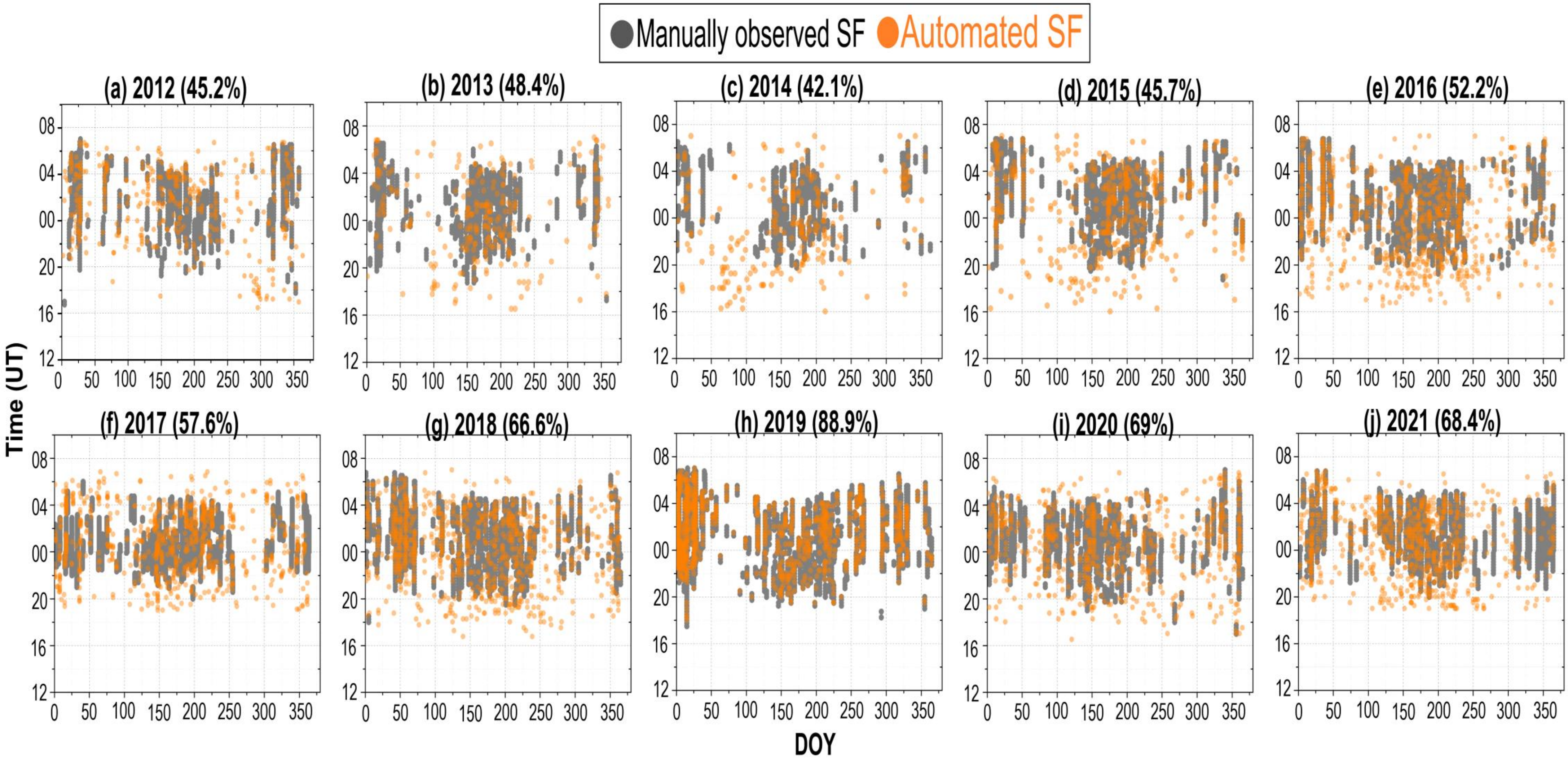

Paul et al (2025), Atmosphere

RESULTS *(35°–40°N latitude)*

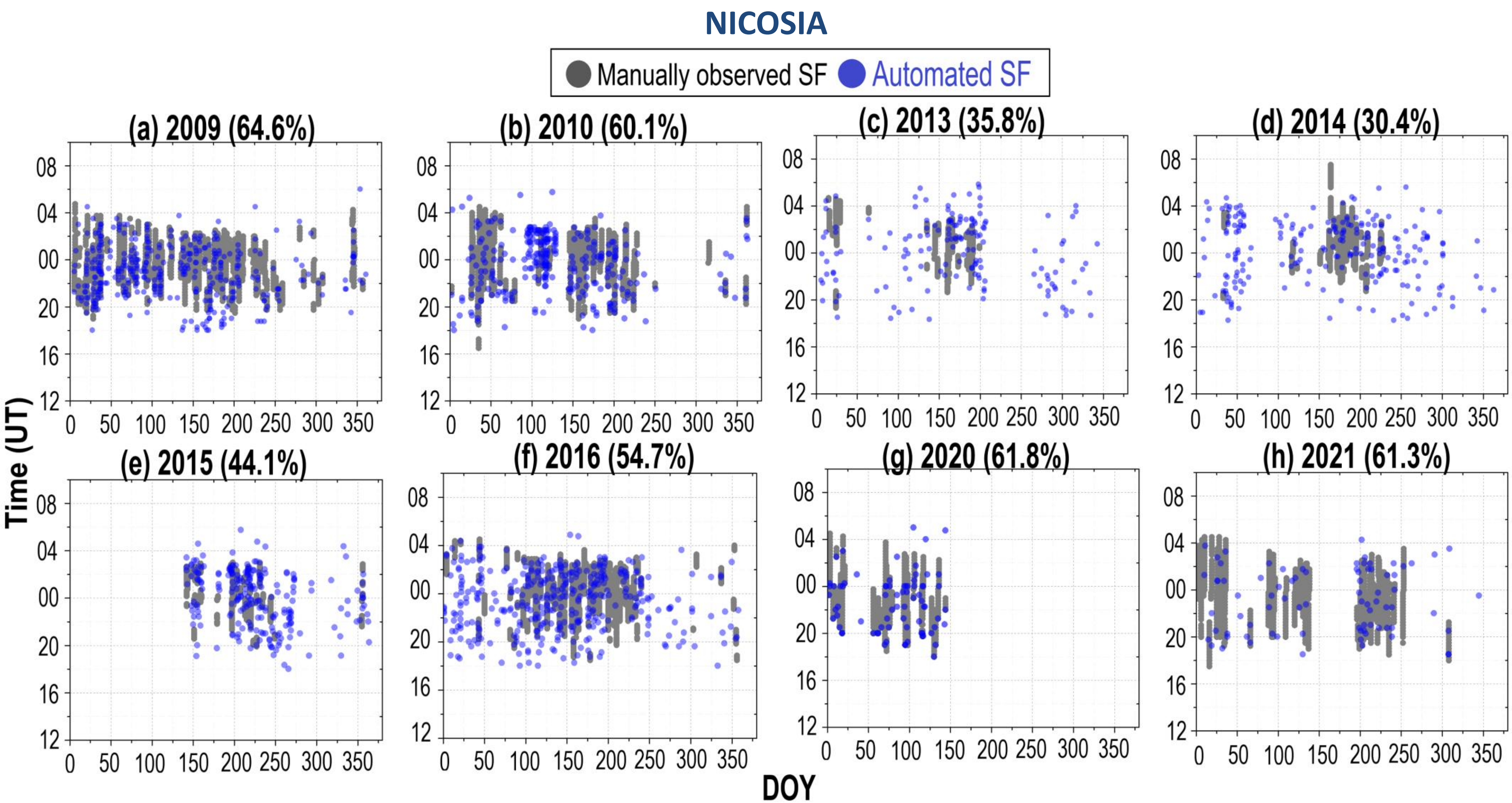

Paul et al (2025), Atmosphere

RESULTS (*Comparative SF occurrences*)

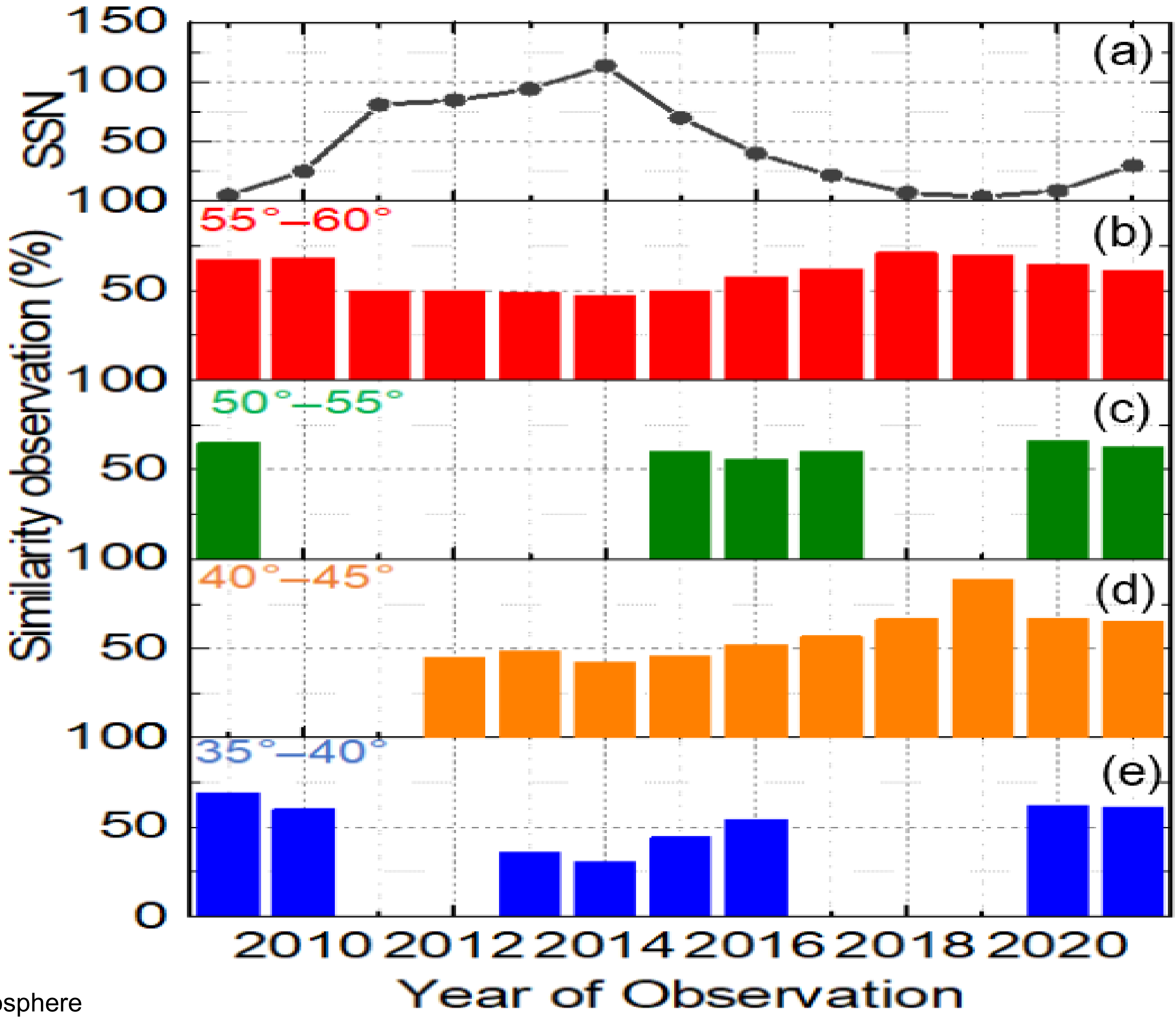

Paul et al (2025), Atmosphere

CONCLUSIONS

- **55°–60°N:** Association between SF_P and SF_M varied from **71% (solar minimum)** to **47% (solar maximum)**. Overestimation during high solar activity was primarily due to **LSTIDs** affecting detection.

- **50°–55°N:** Association varied from **66% to 56%**. Overestimation was most pronounced during **post-sunset hours in equinox and summer**, influenced by **oblique traces** (ionogram) and **MSTIDs**.

- **40°–45°N:** Association varied from **89% to 42%**.
  - Overestimation occurred during **post-sunset equinox and summer** under high solar activity, attributed to **STs** and **MREs**.
  - Underestimation occurred during **summer**, linked to the **spread Es,** obscuring the F-layer trace in ionograms.

- **35°–40°N:** Association varied from **69% to 30%**.
  - Overestimation was observed during **winter** and **high solar activity**, associated with **STs** and **MREs**.
  - Underestimation occurred during **summer**, also related to **spread Es** obscuring F-layer signatures.

- **Systematic effects across latitude sectors:**
  - **Overestimation** of SFP was associated with **LSTIDs, MSTIDs, STs, and MREs**.
  - **Underestimation** of SFP was associated with **spread Es**, which obscured the F-layer trace and led to missed detections.

Acknowledgements

The authors are thankful to **Digital Ionogram DataBase (DIDBase)**, which is part of the **Global Ionospheric Radio Observatory (GIRO) portal (http://giro.uml.edu)**.

Funding for this research was provided by the project "Towards A Global Model for Spread F" – TAGMOS-F, (Ref No: EXCELLENCE/0524/0526) is co-funded by the Republic of Cyprus and the European Regional Development Fund (ERDF) through the 'EXCELLENCE HUBS' Program, in the frame of the Operational Program "ΘΑλΕΙΑ" 2021- 2027.

THANK YOU!

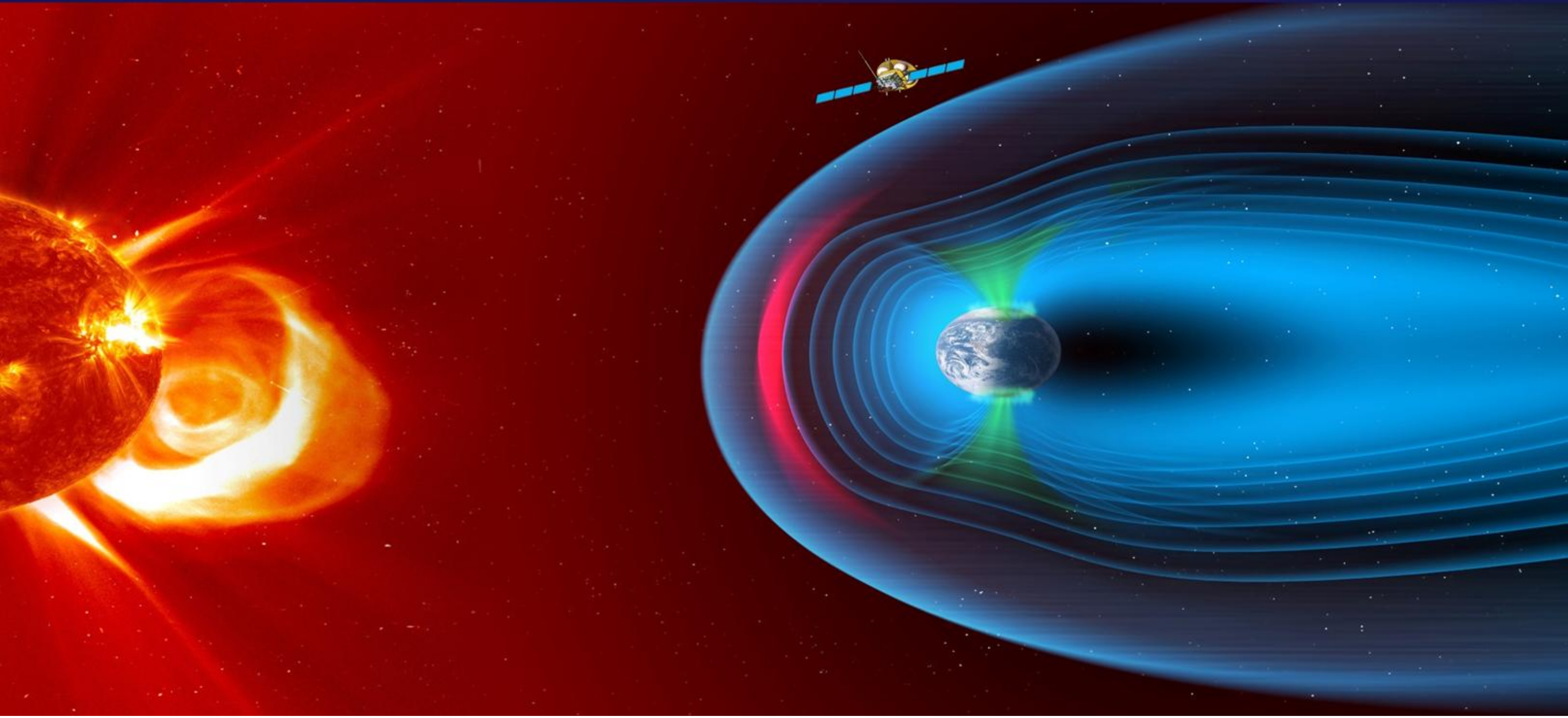

ΘΑΛΕΙΑ 2021-2027
Co-funded by
the European Union
Republic of Cyprus
RESEARCH
& INNOVATION
FOUNDATION
ICTP
The Abdus Salam
International Centre
for Theoretical Physics
IAEA
unesco

INTRODUCTION

Spread F occurrence over Europe in 2017, 2020-2021 (Paul et al. 2023)

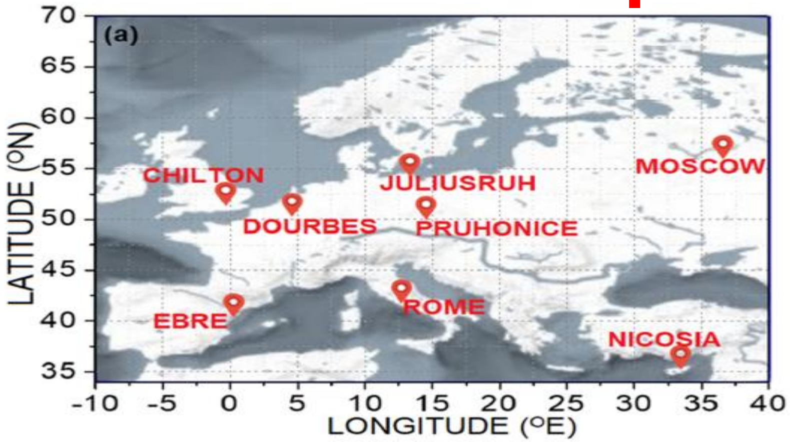

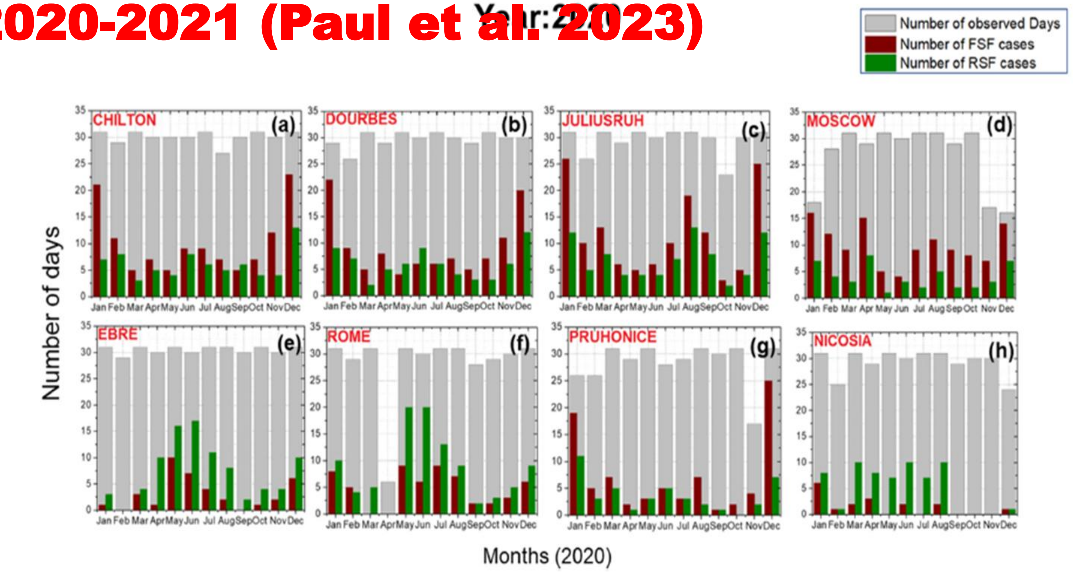

Monthly occurrence rate of FSF and RSF over (a) Chilton (b) Dourbes (c) Juliusruh (d) Moscow (e) Roquetes (f) Rome (g) Pruhonice and (h) Nicosia during 2020.

Station: Rome-Roquetes (Ebre); Date: 17/03/2017-18/03/2017

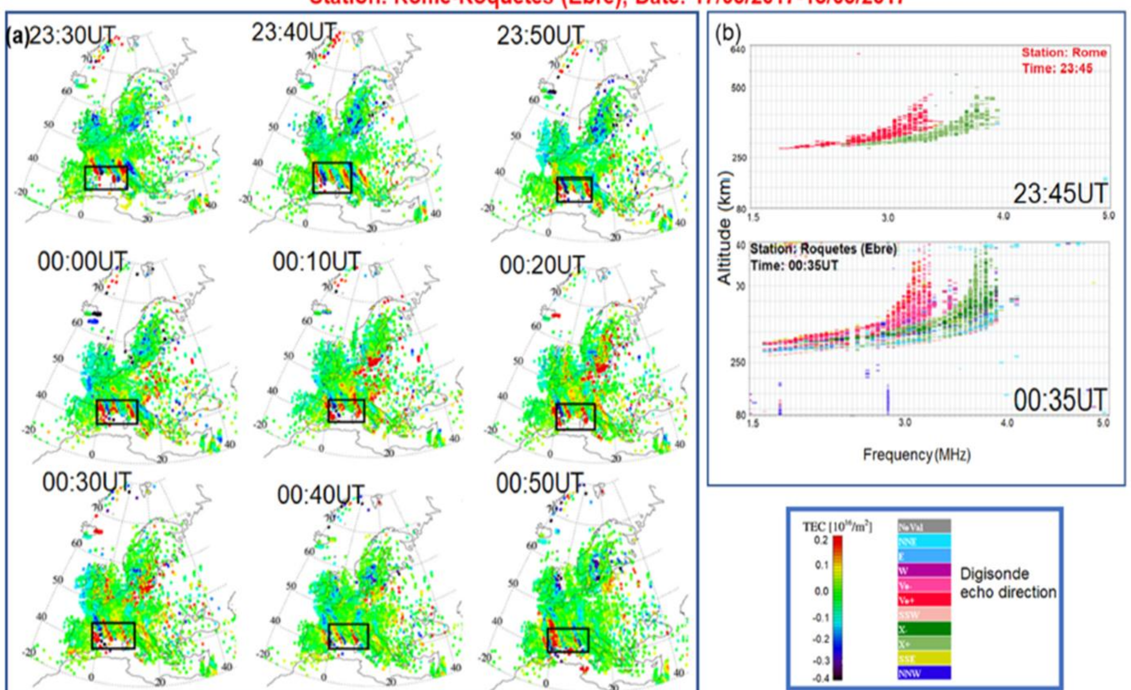

Case of common spread F occurrence between Rome and Roquetes on 17th-18th March 2017 (a) TID wavefront signatures in GPS d-TEC map (b) ionograms over Rome and Roquetes.

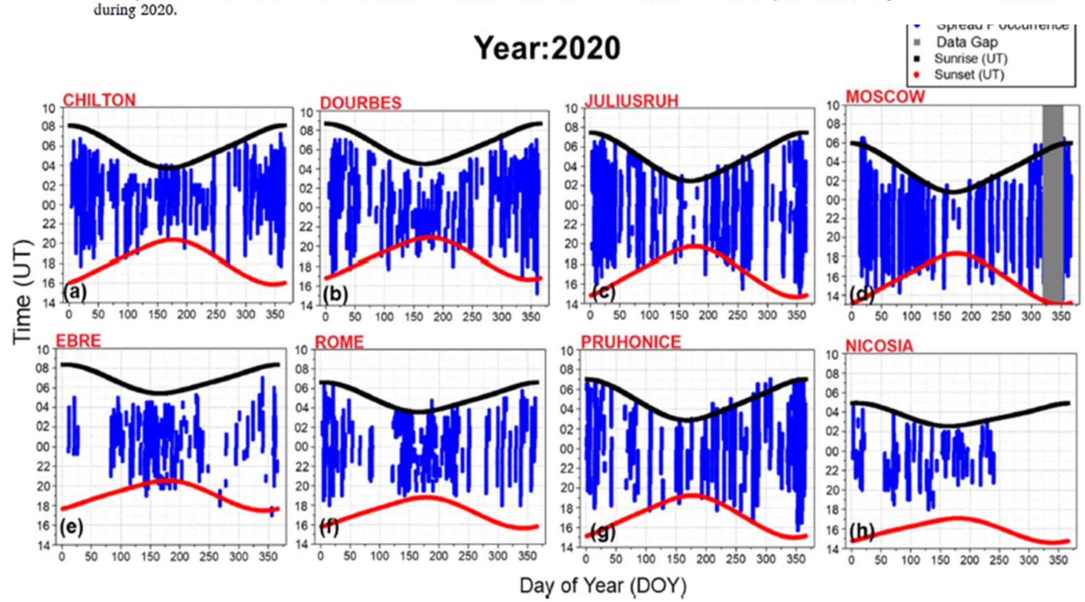

Diurnal occurrence rate of spread F w.r.t. solar terminator over (a) Chilton (b) Dourbes (c) Juliusruh (d) Moscow (e) Roquetes (f) Rome (g) Pruhonice and (h) Nicosia during 2020.